
CONTEXTUAL FEATURE SELECTION WITH CONDITIONAL STOCHASTIC GATES

Ram Dyuthi Sristi
UC San Diego
La Jolla, CA, USA
rsristi@ucsd.edu

Ofir Lindenbaum
Bar-Ilan University
Ramat Gan, Israel
ofirlin@gmail.com

Maria Lavzin, Jackie Schiller
Technion
Haifa, Israel
maria.lavzin@gmail.com,
jackie@technion.ac.il

Gal Mishne
UC San Diego
La Jolla, CA, USA
gmishne@ucsd.edu

Hadas Benisty
Technion
Haifa, Israel
hadasbe@technion.ac.il

ABSTRACT

We study the problem of contextual feature selection, where the goal is to learn a predictive function while identifying subsets of informative features conditioned on specific contexts. Towards this goal, we generalize the recently proposed stochastic gates (STG) Yamada et al. [2020] by modeling the probabilistic gates as conditional Bernoulli variables whose parameters are predicted based on the contextual variables. Our new scheme, termed conditional-STG (c-STG), comprises two networks: a hypernetwork that establishes the mapping between contextual variables and probabilistic feature selection parameters and a prediction network that maps the selected feature to the response variable. Training the two networks simultaneously ensures the comprehensive incorporation of context and feature selection within a unified model. We provide a theoretical analysis to examine several properties of the proposed framework. Importantly, our model leads to improved flexibility and adaptability of feature selection and, therefore, can better capture the nuances and variations in the data. We apply c-STG to simulated and real-world datasets, including healthcare, housing, and neuroscience, and demonstrate that it effectively selects contextually meaningful features, thereby enhancing predictive performance and interpretability.

1 Introduction

Feature selection techniques are commonly used in machine learning to identify informative features from a large set of observed variables. With the acquisition of high-dimensional datasets and the development of complex models across all domains, such schemes are increasingly important in scientific domains and interpretable artificial intelligence. These frameworks help improve interpretability by identifying key features, reduce the complexity of models by eliminating non-informative features, and may lead to better generalization Li et al. [2017], Kumar and Minz [2014], Islam et al. [2022], ?. Feature selection can be broadly categorized into filter, wrapper, and embedded methods.

Filter methods Battiti [1994], Peng et al. [2005], Estévez et al. [2009], Song et al. [2007, 2012], Chen et al. [2017], Sristi et al. [2022] use a predefined criterion independent of the predictive model to rank and select features, for example, statistical measures like correlation or mutual information Lewis [1992]. Wrapper methods Kohavi and John [1997], Stein et al. [2005], Zhu et al. [2007], Reunanen [2003], Allen [2013], on the other hand, use the predictive model itself as a criterion for feature selection. These methods select subsets of features and evaluate the prediction quality only based on those features to identify the subset with the best performance. This can be prohibitively expensive for complex models. Embedded methods Tibshirani [1996], Hans [2009], Li et al. [2011, 2006] incorporate feature selection into the model training process, for example, regularization-based techniques like LASSO and its variants

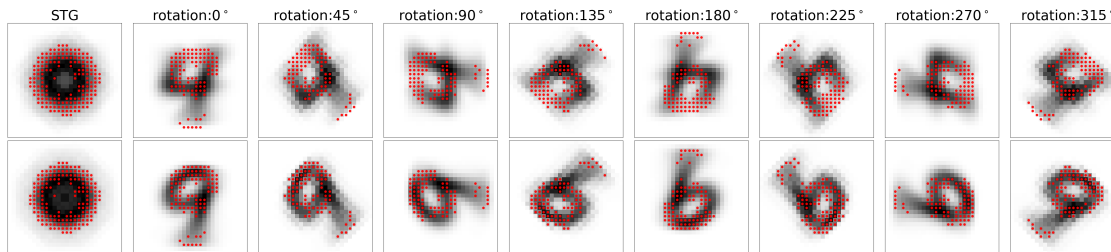


Figure 1: Binary classification between digits 4 (top row) and 9 (bottom row) in the MNIST dataset. We contrast STG feature selection (leftmost column) with c-STG contextual feature selection as conditioned on each rotation angle. Each image depicts the mean pixel values across all rotated images (left) or all images at a given rotation. Red dots indicate the features selected using STG (left) or c-STG for each rotation angle.

Daubechies et al. [2008], Bertsimas et al. [2017]. We develop an embedded method to learn the prediction model and informative features in an end-to-end fashion.

All mentioned feature selection schemes are global and identify one set of informative features for the entire population. However, in many cases, the importance of features varies as a function of contextual information, which does not encode the outcome variable on its own. For example, predicting the likelihood of a patient developing a particular disease in healthcare requires identifying the most important features specific to the patient’s demographics, medical history, and lifestyle Goldstein et al. [2017]. We can identify which explanatory features directly predict the disease risk using feature selection. However, if we take into account context, for example, age or gender, then we can identify whether the relevant explanatory features vary in their significance as a function of context. Thus, certain conditions depend on one subset of explanatory features if the patient is young but on a different subset if the patient is old. In this case, considering context may improve performance, but more importantly, provide valuable information for clinicians. Similarly, product recommendation systems for online shoppers must identify relevant features based on the user’s location, time of day, and device used for shopping Baltrunas and Ricci [2009].

Most feature selection methods are not designed to capture the complex relation between features, context, and the outcome. They either overlook contextual variables or concatenate them with explanatory features when selecting important subsets of features. This limits interpretability as even if the context variables are selected, it does not indicate how the other features depend on them. An alternative is to train a separate model for different values of categorical context variables, e.g., gender, by dividing the data accordingly. However, that increases computation time given multiple categorical contexts and, more importantly, reduces the amount of training data available to train each model, which can limit the performance. Moreover, when the contextual parameter is not categorical but rather continuous (e.g., age, location), training multiple models requires artificial binning of context (age groups, for example). It coarsens the interpretability of feature importance across contexts. Binning the data into categories becomes even more problematic when contextual information includes multiple variables (age and gender, location, and income level).

For illustration purposes, we consider a binary classification task between digits 4 and 9 observed at various rotations (see Fig. 1). Suppose the goal is to select a subset of informative pixels (features) for classifying the two digits. In the original orientation (zero rotation), the pixels on the top of the image are more significant than those at the bottom for distinguishing between 4 and 9. When we rotate the digits by intervals of 45 degrees, global feature selection models will select almost all features as informative. However, given a specific rotation angle, only a subset of these features are informative. Moreover, the rotation angle is unrelated to the response (the identity of the digit). Using rotation as a contextual variable to select the informative pixels for the classification can alleviate overfitting and improve the interpretability of the model. In Figure 1, we present features (pixels) selected by the proposed approach as conditioned on a rotation variable. The significant features rotate as the context changes, and our model identifies the features that best distinguish between digits 4 and 9 for each context. In contrast, the features selected by the global STG Yamada et al. [2020] (Fig. 1 left), trained across all rotated images, mainly recover the action of rotation, without providing meaningful interpretable features for class separation.

In this paper, we propose a method for context-specific feature selection in a supervised learning setup. We assume that the probability that a specific feature is informative follows a conditional Bernoulli distribution. To enable backpropagation through the discrete distribution, we reparametrize the Bernoulli variables using a truncated Gaussian Yamada et al. [2020] whose mean is predicted using a hypernetwork that receives the context variables as input. We learn the weights of the hypernetwork and the weights of a prediction model by empirical risk minimization. Since the hypernetwork is parametric, we can generalize the contextual feature selection prediction to unseen contexts. Our framework enables studying the explainability of the model along two axes: 1) given a context, we identify the importance of the different

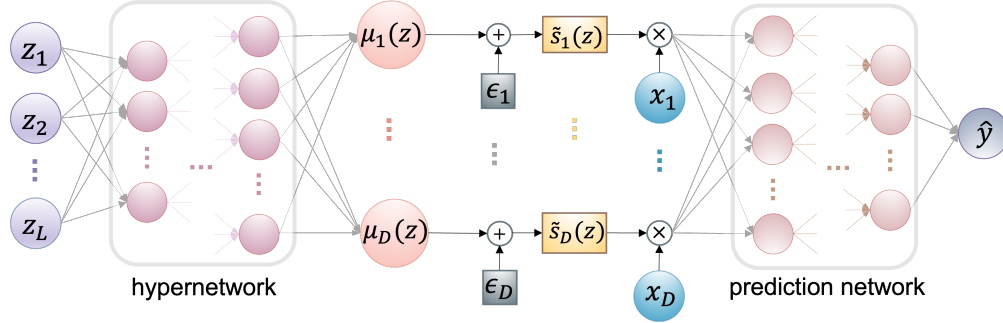


Figure 2: Illustration of our end-to-end contextual feature selection framework. The contextual variables z (purple) are inputs to the hypernetwork, which outputs the STG parameters $\mu(z)$, which, along with ϵ set the status of the gate \tilde{s}_d (yellow) for feature x_d (blue). These are inputs to the prediction model.

features, which is essential for performing an accurate prediction task; and 2) given a feature, we identify how its importance varies across different contexts. Overall, our contributions are as follows:

1. We develop an end-to-end machine learning framework that consists of two networks: a hypernetwork and a prediction network. The hypernetwork maps contextual variables to the probabilistic feature selection parameters, while the prediction network maps explanatory features and their corresponding feature significance to the prediction task.
2. We analyze the optimal risk of c-STG compared with STG and study the optimal solutions under a linear regression prediction model.
3. Empirical results are provided on both simulated and real-world datasets, demonstrating the effectiveness and flexibility of our proposed method compared to existing techniques.

Related Work: Recently, two methods have been proposed for context-specific feature selection: Contextual Explanation Networks (CEN) Al-Shedivat et al. [2020] and contextual LASSO Thompson et al. [2023]. Both calculate feature significance deterministically, while c-STG employs a probabilistic approach. In terms of selecting a sparse set of features, CEN lacks sparsity-related constraints, and contextual LASSO uses an L_1 regularization, which suffers from coefficient shrinkage. In contrast, c-STG adopts stochastic gates regularization, closely approximating the L_0 sparsity constraint, conditioned on context. Both methods are confined to linear prediction models, although contextual LASSO uniquely modulates linear model parameters based on context. In contrast, our c-STG supports both linear and non-linear prediction models.

Another line of research focuses on sample-wise (instance-wise) feature selection techniques Chen et al. [2018], Yoon et al. [2018], ? and active methods Shim et al. [2018], Covert et al. [2023]. Unlike traditional population-level and context-grouped methods, sample-wise methods capture specific features for individual points. A disadvantage is that all feature values need to be known apriori for a new sample, which limits applicability in specific settings, e.g., health. Active selection, prioritizing real-time acquisition, iteratively chooses features per sample. While these methods do not address contextual feature selection directly, they can be adapted to context in the following manner. For active feature selection, the contextual variables will be pre-selected, and then the significant features are selected in an online manner. For sample-wise selection, the contextual variables are always selected. To interpret feature selection as a function of context, it would be necessary to aggregate the selected features across all samples for a given context value, thus resorting to coarse binning. In contrast, our c-STG method identifies key features as a function of context, and can implicitly extend to unseen context values, e.g., an age value not seen in the training data.

2 Problem Setup and Background

Let $X \subseteq \mathbb{R}^D$, $Z \subseteq \mathbb{R}^L$ and $Y \subseteq \mathbb{R}$ be the random variables corresponding to the input explanatory features, input contextual variables, and output prediction value respectively. Given the realizations of these random variables from some unknown joint data distribution $P_{X,Z,Y}$, the goal of embedded contextual feature selection methods is to achieve the following simultaneously: 1) construct a hyper-model $h_\phi : \mathbb{R}^L \rightarrow \{0, 1\}^D$ that selects a subset of explanatory features X_S as a function of context z ; and 2) construct a model $f_\theta : \mathbb{R}^D \rightarrow \mathbb{R}$ that predicts the response Y based on

these selected features. Given a loss function L , we solve for the parameters θ and ϕ of the risk minimization problem

$$R(\theta, \phi) = \mathbb{E}_{X,Z,Y}[L(f_\theta(x \odot s(z)), y)] \quad , \quad s(z) = h_\phi(z), \quad (1)$$

where x, z and y represent a realization of the random variables X, Z and Y following a data distribution $P_{X,Z,Y}$, the feature selection vector, given by a vector of indicator variables for the set \mathcal{S} , is the output of the hypernetwork $s(z) = h_\phi(z) = \{0, 1\}^D$, and \odot denotes the point-wise product.

3 Conditional STG

The risk minimization in (1) often includes an additional constraint to induce sparsity on the feature selection, for example, $\|s\|_0 \leq D$, which reduces the number of selected features and enhances interpretability. Model interpretability is crucial for understanding complex relations between input features and the predicted target in applications such as health care Liu et al. [2019], shopping Baltrunas and Ricci [2009], and neuroimaging data Levy et al. [2020].

In practice, the ℓ_0 regularization is known to be computationally expensive and intractable for high-dimensional data. Additionally, it is impossible to incorporate the ℓ_0 norm into gradient descent-based optimization, e.g., as used in deep networks. Here, we propose a probabilistic and computationally efficient approach promoting contextual feature selection by implementing ℓ_0 regularization applied to stochastic gates, which mask the input feature conditioned on the context.

First, we introduce conditional Bernoulli gates corresponding to each of the D features as a probabilistic extension of contextual feature selection. Expressly, we assume that the probability of an individual explanatory feature being selected, given contextual features z , follows a Bernoulli distribution independent of the probability of selecting other explanatory features. Let $S'|Z$ be a conditional random vector that represents these independent Bernoulli gates, with $\mathbb{P}(S'_d = 1|Z = z) = \pi_d(z)$ for $d \in [D]$, and let $s'(z) = s'|z$ be a realization of the random vector $S'|Z$. We term these conditional-Stochastic Gates (c-STG), as the parameter of the distribution of each gate is conditional on the context variables z .

The hypernetwork h'_ϕ learns a parametric function mapping the contextual variable z to the conditional probability, i.e., the parameter of the Bernoulli distribution. The task of contextual variable selection then boils down to learning the parameters $\pi_d(z) = h'_\phi(z)$ of this conditional distribution, which spans over a continuous space $[0, 1]^D$, instead of a discrete set $\{0, 1\}^D$, as in Eq. 1. Let $h'_\phi : \mathbb{R}^L \rightarrow [0, 1]^D$ be the function that maps the contextual information to the parameters of the probability distribution. This reformulates the regularized version of the risk in Eq.(1) to

$$\hat{R}(\theta, \phi) = \hat{\mathbb{E}}_{X,Z,Y} \mathbb{E}_{S'|Z} [L(f_\theta(x \odot s'(z)), y) + \lambda \|s'(z)\|_0] \quad \text{where} \quad \pi(z) = h'_\phi(z) \quad (2)$$

where $\hat{\mathbb{E}}_{X,Z,Y}$ represents the empirical expectation over the observations X, Z and Y and $\mathbb{E}_{S'|Z} \|s'(z)\|_0 = \sum_{d=1}^D \pi_d(z)$, the sum of Bernoulli parameters. Note that if we constrain $\pi_d \in \{0, 1\}$, this formulation is equivalent to the cardinality-constrained version of Eq. (1), with a regularized penalty on cardinality rather than an explicit constraint. Moreover, this probabilistic formulation converts the combinatorial search to a search over the space of Bernoulli distribution parameters. Thus, the problem of feature selection translates to finding θ^* and ϕ^* that minimize the empirical risk based on the formulation in (2).

3.1 Bernoulli Continuous Relaxation for Contextual Feature Selection

While it is appealing to incorporate discrete random variables into a differentiable loss function designed to retain the informative features in the data, the gradient estimates of discrete random variables tend to suffer from high variance He and Niyogi [2004]. Therefore, recent work has proposed continuous approximations of discrete random variables Maddison et al. [2016], Jang et al. [2016]. One popular approach for continuous relaxation is based on the Gaussian distribution. This approach is more stable in feature selection than Gumbel-softmax-based techniques like concrete and hard concrete Jang et al. [2016], which can induce high variance in the approximation of Bernoulli variables Yamada et al. [2020], Jana et al. [2021]. Such relaxations Louizos et al. [2017] have been used for many applications, including discrete softmax activations Jang et al. [2016], feature selection Yamada et al. [2020], Lindenbaum et al. [2021c], Shaham et al. [2022], and sparsification Lindenbaum et al. [2021b,a]. Here, we use a Gaussian-based relaxation of the Bernoulli variables, termed Stochastic Gates (STG) Yamada et al. [2020], which is differentiated based on the reparameterization trick Miller et al. [2017], Figurnov et al. [2018].

The Gaussian-based continuous relaxation for the Bernoulli variable is defined as $\tilde{s}_d(z) = \max(0, \min(1, \mu_d(z) + \epsilon_d))$, where ϵ_d is drawn from a normal distribution $\mathcal{N}(0, \sigma^2)$, with σ fixed throughout training. Unlike the ReLU function, which only clips the negative values and sets them to zero, the mean-shifted Gaussian variable clips both the positive

and negative values, therefore, accounts for the binary nature of the original random variable. Here, we learn μ_d as a parametric function of the contextual variables z . Thus, the hypernetwork \tilde{h}_ϕ aims to learn the parameters of the relaxed-continuous distribution as a function of the context variables z instead of learning the original discrete distribution. Our objective as a minimization of the empirical risk $\hat{R}(\theta, \phi)$ is as follows:

$$\min_{\theta, \phi} \hat{\mathbb{E}}_{X, Z, Y} \mathbb{E}_{\tilde{S}|Z} [L(f_\theta(x \odot \tilde{s}(z)), y) + \lambda \|\tilde{s}(z)\|_0] \quad \text{where} \quad \mu(z) = \tilde{h}_\phi(z) \quad (3)$$

where $\tilde{S}|Z$ is a random vector with D independent variables $\tilde{s}_d(z) = s|z$ for $d \in [D]$. The regularization term can be further simplified to

$$\mathbb{E}_{\tilde{S}|Z} \|\tilde{s}(z)\|_0 = \sum_{i=1}^D \mathbb{P}(\tilde{s}_d(z) > 0) = \sum_{d=1}^D \Phi\left(\frac{\mu_d(z)}{\sigma}\right), \quad (4)$$

where Φ is the standard Gaussian CDF. The term (4) penalizes open gates so that gates corresponding to features that are not useful for prediction are encouraged to transition into a closed state (which is the case for small $\mu_d(z)$). Hence, we perform a context-specific feature selection strategy by inducing sparsity through the empirical mean of the regularization term (4) over multiple realizations of Z . This enables us to select distinct informative features for different contexts while maintaining the sparsity.

In practice, we consider the function class for \tilde{h}_ϕ and f_θ to be a class of neural networks parameterized by ϕ and θ , respectively. To optimize for these parameters, we use a Monte Carlo sampling gradient estimator of (3), which gives

$$\frac{\partial \hat{R}(\theta, \phi)}{\partial \theta} = \frac{1}{K} \sum_{k=1}^K \frac{\partial}{\partial \theta} L(f_\theta(x^{(k)} \odot \tilde{s}(z^{(k)}), y^{(k)})) \quad (5)$$

$$\frac{\partial \hat{R}(\theta, \phi)}{\partial \phi} = \frac{1}{K} \sum_{k=1}^K L'(\tilde{s}(z^{(k)})) \frac{\partial \tilde{s}(z^{(k)})}{\partial \phi} + \lambda \frac{\partial}{\partial \phi} \Phi\left(\frac{\tilde{h}_\phi(z^{(k)})}{\sigma}\right) \quad (6)$$

Here, K represents the number of Monte Carlo samples (corresponds to the batch size). Our methodology is summarized in Algorithm 1 and illustrated in Fig. 2.

During the initial training phase, all gates should have an equal probability of being open or closed. To achieve this, we must set $\mu_d(z) = 0.5 \forall i = 1, 2, \dots, d$ so that all gates approximate a "fair" Bernoulli variable. The initialization of the hyper-model's ϕ using Xavier initialization Glorot and Bengio [2010] and a Sigmoid activation function in the final layer of \tilde{h}_ϕ ensures that the means ($\mu_d(z)$) are centered around 0.5, $\forall z$, early in the training phase. It is worth noting that we need the noise term only during the training phase.

3.2 Theoretical Analysis

In this study, we conduct a thorough theoretical analysis to establish the equivalence between our probabilistic formulation, as represented by Eq.2, and the original NP-hard contextual variable selection problem defined in Eq.1. Additionally, we provide proof demonstrating that c-STG achieves a lower risk than STG. Furthermore, we extend our analysis to a linear regression scenario, where we demonstrate the main advantage of c-STG over STG. While STG selects features with consistent significance across contextual variables on average, c-STG adapts the feature selection process according to the contextual variables, thus effectively learning the optimal feature selection as a function of these variables.

Theorem 1. *Let $s^*(z)$ and $s'^*(z)$ represent the optimal feature selection functions in Eq. 1 and its corresponding probabilistic formulation in Eq. 2 respectively. Then $s^*(z) = s'^*(z)$.*

The proof is provided in the appendix. This theorem suggests that a deterministic search for feature selection can be transitioned to a probabilistic approach. We then use the universal function approximators, deep networks, to learn the function $s'^*(z)$. In subsequent theorems, we contrast c-STG's and STG's performance and feature selection abilities. In Yamada et al. [2020], the optimization problem of the global feature selection using STG is given by

$$\min \hat{\mathbb{E}}_{X, Y} \mathbb{E}_{S'} [L(f_\theta(x \odot s'), y) + \lambda \|s'\|_0], \quad (7)$$

where S' is a random vector that represents independent Bernoulli gates, $\mathbb{P}(S'_d = 1) = \pi_d$ for $d \in [D]$, and s'_d denotes the realization of the random vector S'_d . Note that S' is similar to $S'(z)$ except that the latter is a function of z , and the former is constant for all z . Thus, their approach optimizes for a fixed feature selection independent of contextual information by promoting sparsity in feature selection through the regularization term $\mathbb{E}_{\tilde{S}} [\|\tilde{s}\|_0]$. In contrast, we perform context-specific feature selection by maximizing the sparsity through the empirical mean of Eq. 4 across various realizations of Z . The following theorem draws a connection between their empirical risk minimizations.

Algorithm 1 Proposed Methodology**Input:** $x^{(k)} \in \mathbb{R}^D, z^{(k)} \in \mathbb{R}^L, y^{(k)} \in \mathbb{R}$, for $k = 1, 2, \dots, K$ **Output:** Trained models f_θ and \tilde{h}_ϕ .

- 1: Initialize: $\theta^{(0)}$ and $\phi^{(0)}$ using Xavier initialization.
- 2: Forward Pass:
- 3: **for** $k = 1$ to K **do**
- 4: $\mu(z^{(k)}) = \tilde{h}_{\phi^{(t)}}(z^{(k)})$,
- 5: **where** $\mu(z^{(k)}) = [\mu_1(z^{(k)}), \mu_2(z^{(k)}), \dots, \mu_D(z^{(k)})]$
- 6: **for** $d = 1$ to D **do**
- 7: $\epsilon_d \sim \mathcal{N}(0, \sigma)$
- 8: $\tilde{s}_d(z^{(k)}) = \max(0, \min(1, \mu(z^{(k)}) + \epsilon_d))$.
- 9: **end**
- 10: $\tilde{s}(z^{(k)}) = [\tilde{s}_1(z^{(k)}), \tilde{s}_2(z^{(k)}), \dots, \tilde{s}_D(z^{(k)})]$
- 11: $\hat{y}^{(k)} = f_{\theta^{(t)}}(x^{(k)} \odot \tilde{s}(z^{(k)}))$
- 12: **end**
- 13: Compute empirical risk $\hat{R}(\theta, \phi)$ using Eq. 3
- 14: Back Propagation:
- 15: Update θ : $\theta^{(t+1)} = \theta^{(t)} - \eta \frac{\partial \hat{R}(\theta, \phi)}{\partial \theta} \Big|_{\theta^{(t)}} \quad$ (using Eq. (5))
- 16: Update ϕ : $\phi^{(t+1)} = \phi^{(t)} - \eta \frac{\partial \hat{R}(\theta, \phi)}{\partial \phi} \Big|_{\phi^{(t)}} \quad$ (using Eq. (6))

Theorem 2. *c-STG attains an optimal risk lower or equal to the risk attained by STG.*

Proof: The feasible solution space of STG is contained in the feasible solution space of c-STG as the parameters of the stochastic gates in c-STG can be any function of contextual variables z , which includes a constant function, which is the case in STG. Therefore, the optimal risk attained by c-STG must be less than or equal to the optimal risk value attained by STG.

Through the following theorems 3 and 4, we further emphasize the significance of c-STG over STG.

Theorem 3. *In a linear regression setup, the relationship between the optimal parameters of the conditional Bernoulli stochastic gates, $\pi^*(z)$, and the optimal parameters of the non-parametric Bernoulli stochastic gates π_{stg}^* is given by*

$$\pi_{stg}^* = E_Z[\pi^*(z)]. \quad (8)$$

Theorem 4. *In a linear regression setup, the relationship between the optimal parameters of the conditional Gaussian stochastic gates, $\mu^*(z)$, and the optimal parameters of the non-parametric Gaussian stochastic gates μ_{stg}^* is given by*

$$\mu_{stg}^* = E_Z[\mu^*(z)]. \quad (9)$$

The theorems provided elucidate that c-STG offers an enhanced feature selection resolution by pinpointing features crucial to specific contexts. This stands in contrast to STG, which tends to select features based on their average importance across various contexts. Theorem 3 delineates this difference in the realm of discrete probability spaces, whereas Theorem 4 addresses the continuous probability spaces.

4 Experiments

We evaluate c-STG against a diverse set of benchmarks: 1) context-specific techniques Contextual LASSO and CEN; 2) the sample-specific method INVASE Yoon et al. [2018]; 3) an active feature selection approach: AFS Covert et al. [2023]; 4) population-level methods like LASSO and STG; and 5) a prediction model without any feature selection. We train the population-level methods and prediction model without any feature selection using 1) only the explanatory features as input or 2) concatenating these features with the context variables (referred to as ‘with context’). See the supplementary material for implementation details on the hyper-parameters of all methods. We compare with the sample-specific method INVASE only for the classification setup.¹ We report the performance of all methods in Table 1 and their corresponding number of selected features in the appendix (Table 2) for four datasets, demonstrating c-STG outperforms competing methods, and discuss the interpretability of our contextual feature selection below.

¹Yoon et al. [2018] do not report results on regression, and their code does not include a regression option.

Table 1: Comparison of feature selection on XOR, MNIST, Housing, and heart disease datasets. **Bold** indicates best performance and underline indicates second-best.

	XOR	MNIST	Heart disease	Housing
	Accuracy (%)	Accuracy (%)	Accuracy (%)	R^2 score
LASSO	50.09 (1.23)	83.87 (0.05)	83.50 (3.69)	0.2161 (0.0014)
with context	50.05 (1.09)	83.88 (0.04)	83.67 (3.48)	0.2272 (0.0016)
Prediction model	70.74 (17.72)	98.11 (0.05)	86.53 (1.51)	0.2022 (0.0361)
with context	71.93 (11.88)	98.21 (0.07)	83.92 (5.52)	0.2132 (0.0381)
STG	51.54 (0.90)	<u>98.55</u> (0.08)	86.53 (2.11)	0.2139 (0.0023)
with context	51.45 (0.95)	<u>98.34</u> (0.07)	87.88 (1.95)	0.2234 (0.0022)
CEN	50.08 (0.67)	87.66 (0.24)	84.17 (5.69)	0.2561 (0.0002)
Contextual LASSO	50.18 (0.42)	97.17 (0.04)	83.19 (5.32)	0.4616 (0.0033)
AFS	78.95 (19.91)	94.83 (0.84)	86.44 (1.07)	0.3963 (0.0092)
INVASE	52.36(1.70)	88.06(2.30)	87.22(2.20)	-
c-STG (Ours)	100 (0)	98.66 (0.05)	87.55 (3.41)	0.3976 (0.0082)

Simulated Dataset: First, we use synthetic data to validate that our method can identify context-specific informative features while learning complex non-linear prediction functions. Following synthetic examples in Yamada et al. [2020], Yang et al. [2022], we design a moving XOR dataset as

$$\text{Moving XOR: } y = \begin{cases} \mathbf{x}_1 \times \mathbf{x}_2, & \text{if } T = -1, \\ \mathbf{x}_2 \times \mathbf{x}_3, & \text{if } T = 0, \\ \mathbf{x}_3 \times \mathbf{x}_4, & \text{if } T = 1, \end{cases} \quad (10)$$

We generate a data matrix X with $3N = 1500$ samples and 20 features, where each entry is sampled from a fair Bernoulli distribution ($P(x_{ij} = 1) = P(x_{ij} = -1) = 0.5$). The contextual variable T is trinary, with $T = -1$ for the first N samples, $T = 0$ for the second N samples, $T = 1$ for the last N samples. Based on the value of T , the response variable y for different samples will have different subsets of features. In Fig. 3 c-STG correctly recovers the dependence of y on the features as a function of T .

MNIST: We apply our proposed contextual feature selection approach for image classification using a subset of the MNIST dataset, including digit images of 4 and 9. To create a contextually diverse set of input images, we rotate each original image in eight different directions at equal intervals, covering 360 degrees, resulting in eight distinct images per original image. The goal is to identify the pixels that most effectively differentiate between the digits for a given rotation. When applying c-STG, we represent the rotation as an eight-dimensional one-hot encoded input to the hypernetwork. We trained a classifier with this hyper-parameter setting, resulting in a test accuracy of 98%. In Fig. 1, we contrast STG with c-STG, illustrating the superiority of context-specific feature selection over population-level analysis. By comparing separate STG models for distinct categorical contexts against a unified c-STG model, we find that c-STG leads to higher accuracy with fewer samples(Fig.9).

Heart disease dataset: We now focus on medical data, specifically, the heart disease dataset from UCI ML repository Janosi et al. [1988]. Given features including chest pain type, resting blood pressure, serum cholesterol levels, and more, our goal is to understand how age and gender influence these biometrics in relation to the risk of heart disease. Age and gender are set as a two-dimensional contextual input to our hypernetwork in this binary classification problem. Table 1 shows the 5-fold cross-validation accuracy where we surpass other contextual methods. While STG with context achieves the best performance, it lacks the interpretability provided by c-STG, as shown below.

Analysis of c-STG’s gate values conditioned on gender and age (Fig. 4) highlights the significance of specific factors relative to age and gender. For instance, we observe that cholesterol levels (‘chol’) play a more significant role in males aged 30-50 compared to those aged 50-70, suggesting the importance of closely monitoring cholesterol during the earlier age range, which could be because mid-life males are in a stage of life where they typically may have higher metabolic activity and are more prone to developing heart conditions associated with elevated cholesterol levels. Females aged 30-50 show a higher importance of having a normal resting electrocardiographic result (‘restecg0’), indicating a healthy heart rhythm compared to females aged 50-70. This difference may be attributed to the younger

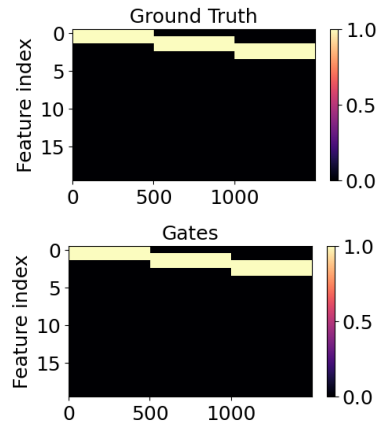


Figure 3: Moving XOR. Ground truth (top) informative features as a function of T . Features identified by c-STG (bottom).

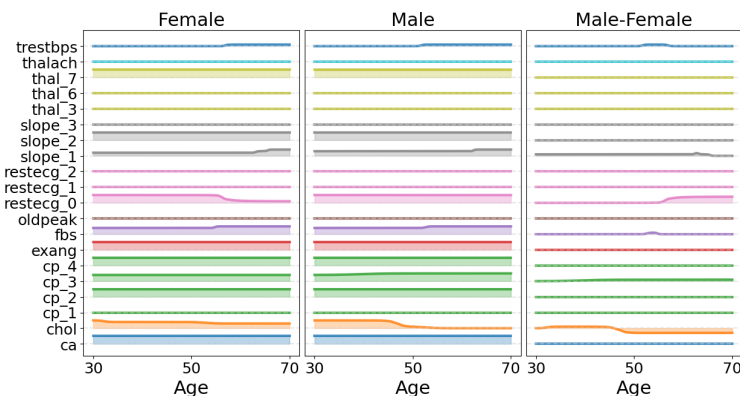


Figure 4: Heart disease. We plot the c-STG values (line 10 from Algorithm 1) for each input feature as a function of age conditioned on females (left) and males (center). The difference in the c-STG values between male and female contexts shows gender-specific differences as a function of age.

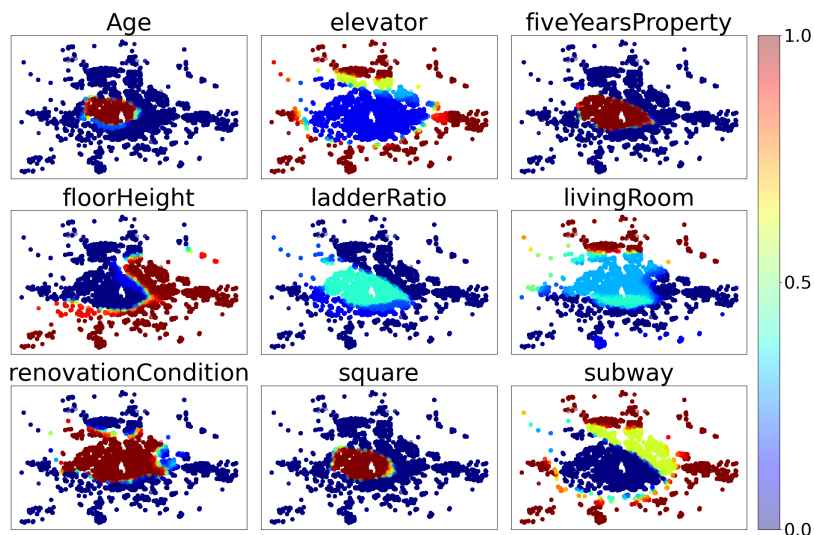


Figure 5: Housing. The c-STG feature selection probabilities as a function of location for each of the nine features. Red (Blue) indicates that the features are selected (removed).

age group’s reproductive years and increased physical activity. While maintaining optimal heart health is essential throughout life, our results highlight the varying importance of certain factors based on age and gender.

Housing dataset: In the domain of housing price prediction, understanding how the renovation condition of a house influences its cost based on the location of the house in the city requires context-specific feature selection. The Housing dataset Lianjia [2017] includes various features such as age, elevator, floor height, renovation condition, and the latitude and longitude of the house. Our goal is to predict the price of the house using all the features while considering the location information as contextual data. Thus, the latitude and longitude are set as a two-dimensional contextual input to our hypernetwork. On this dataset with a linear prediction model, c-STG outperforms CEN, but contextual LASSO performs better than c-STG due to its enhanced model capacity. It learns not only context-specific feature importance but also context-specific weights, setting it apart from c-STG’s linear model. However, its capacity is limited to linear predictions without support for non-linear models, leading to poor performance on other datasets. Visualizing the c-STG gate values as a function of location in Fig. 5 reveals interesting insights into the Housing dataset. First, the importance of explanatory features is localized, with neighboring locations exhibiting similar feature significance. Second, we discovered that the center of the city has a higher significance for age, renovation conditions, and whether the owner owned the property for less than five years (‘fiveYearsProperty’) compared to the outskirts, while the presence of an elevator and subway is more critical in the outskirts than in the center of the city. These findings provide valuable

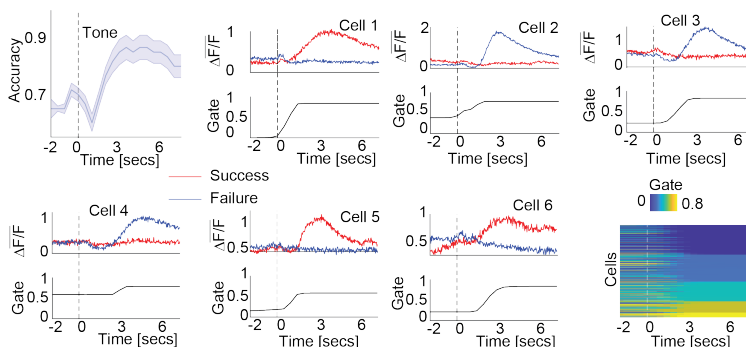


Figure 6: Neuroscience dataset. Top left - prediction accuracy as a function of time; Blue and red traces - average activity (across success and failure trials, respectively) of six cells, whose corresponding gates are open; bottom right - gate values for all cells vs. time.

insights for real estate companies and policymakers. By understanding which features are more important in which locations, they can make better-informed decisions regarding housing prices, regulations, and development.

Neuroscience: For neuroscience applications, feature selection can aid in model interpretability. In studying how the brain encodes behavior, perception, and memory, machine learning models are trained to predict measures of behavior from neuronal activity recordings. Feature selection can reveal individual (or subsets of) neurons encoding a particular behavior as a function, e.g., the animals' task-relevant timing or arousal state. In Levy et al. [2020], the authors study a motor task where mice learn a hand-reach task of a food pellet, given an auditory cue (tone, over multiple weeks). They recorded the activity of neurons in layers 2-3 of the primary motor cortex (M1), and each trial of the animal was labeled as successful if the animal managed to grab and eat the food pellet. Learning a new motor task through repeated trials is a dynamic process; the brain processes the difference between the desired and actual movement and estimates the required correction for the next attempt to achieve improvement. Therefore, cellular networks in the motor cortex are expected to communicate error signals while acquiring a new motor task. To test this hypothesis, Levy et al. [2020] trained an SVM binary classifier per neuron to classify trials as success or failure based on the average activity of the neuron within a short time window during the trial. This resulted in training 7866 models (342 neurons \times 23 sliding time windows). This analysis showed that 1) outcome can be consistently decoded from neuronal activity starting 2 seconds after the tone till the end of the trial; 2) 12% of neurons exhibited prolonged activity starting 2 seconds after the tone, on either success or on failure trials, thus "reporting" the outcome of the trial. Using a single c-STG model, we can reveal the same biological findings. We set the prediction model to be a classifier; the explanatory features are the neuronal activity of all neurons in a given time window, and the contextual variable is time. Fig. 6 presents our model's (test) accuracy rate as a function of time, indicating that performance was successfully classified starting from 2 seconds after the tone. We also plot the activity of 6 neurons selected as informative by the hypernetwork, where the time traces are averaged across successful and failed trials, along with the value of their corresponding gate (raw activity of these neurons in all trials is plotted in the supplemental). The value of the gates across time identifies 2 seconds after the tone as a transition for this network where 17% of gates are open (> 0.5). Overall, c-STG captured the complex dynamics of how the outcome is encoded within the neuronal activity of the ensemble of neurons. C-STG was able to detect individual neurons reporting outcome as a function of time using a single model, a biological finding which Levy et al. [2020] used thousands of SVM models to reveal.

5 Conclusion

In this paper, we presented an embedded method for context-specific feature selection. We developed conditional stochastic gates, which use a hypernetwork to map between contextual variables and the parameters of the conditional distribution, which can be paired with either linear or non-linear predictive models. This leads to improved accuracy and interpretability of the model. Our c-STG efficiently determines which input features are relevant for prediction within a single trained model for categorical, continuous, and/or multi-dimensional context. We demonstrate that our method outperforms embedded feature selection methods and reveals insights across multiple domains. A limitation of our work is the challenge of parameter tuning, specifically the regularization, and cross-validation is often necessary to find optimal value. It is worth noting that LASSO has a well-established theory for tuning its λ parameter. Developing automated procedures for parameter tuning for c-STG would be an exciting avenue for future research. Additionally, we plan to refine c-STG to learn both linear and non-linear prediction model parameters based on context.

6 Acknowledgements

This research is partially supported by a Simons Foundation Pilot Award - 876513SPI (G.M. and R.S.) and Israel Science Foundation 1432/19 (J.S.)

References

- Maruan Al-Shedivat, Avinava Dubey, and Eric P. Xing. Contextual explanation networks, 2020.
- Genevera I Allen. Automatic feature selection via weighted kernels and regularization. *Journal of Computational and Graphical Statistics*, 22(2):284–299, 2013.
- Linas Baltrunas and Francesco Ricci. Context-based splitting of item ratings in collaborative filtering. In *Proceedings of the third ACM conference on Recommender systems*, pages 245–248, 2009.
- Roberto Battiti. Using mutual information for selecting features in supervised neural net learning. *IEEE Transactions on neural networks*, 5(4):537–550, 1994.
- Dimitris Bertsimas, Martin S. Copenhaver, and Rahul Mazumder. The trimmed lasso: Sparsity and robustness, 2017.
- Jianbo Chen, Mitchell Stern, Martin J Wainwright, and Michael I Jordan. Kernel feature selection via conditional covariance minimization. In *Advances in Neural Information Processing Systems*, pages 6946–6955, 2017.
- Jianbo Chen, Le Song, Martin Wainwright, and Michael Jordan. Learning to explain: An information-theoretic perspective on model interpretation. In *International conference on machine learning*, pages 883–892. PMLR, 2018.
- Ian Connick Covert, Wei Qiu, Mingyu Lu, Na Yoon Kim, Nathan J White, and Su-In Lee. Learning to maximize mutual information for dynamic feature selection. In *International Conference on Machine Learning*, pages 6424–6447. PMLR, 2023.
- Ingrid Daubechies, Ronald DeVore, Massimo Fornasier, and C. Sinan Gunturk. Iteratively re-weighted least squares minimization for sparse recovery, 2008.
- Pablo A Estévez, Michel Tesmer, Claudio A Perez, and Jacek M Zurada. Normalized mutual information feature selection. *IEEE Transactions on Neural Networks*, 20(2):189–201, 2009.
- Mikhail Figurnov, Shakir Mohamed, and Andriy Mnih. Implicit reparameterization gradients. In *Advances in Neural Information Processing Systems*, pages 441–452, 2018.
- Xavier Glorot and Yoshua Bengio. Understanding the difficulty of training deep feedforward neural networks. In *Proceedings of the thirteenth international conference on artificial intelligence and statistics*, pages 249–256. JMLR Workshop and Conference Proceedings, 2010.
- Benjamin A Goldstein, Ann Marie Navar, Michael J Pencina, and John PA Ioannidis. Opportunities and challenges in developing risk prediction models with electronic health records data: a systematic review. *Journal of the American Medical Informatics Association: JAMIA*, 24(1):198, 2017.
- Chris Hans. Bayesian Lasso regression. *Biometrika*, 96(4):835–845, 2009.
- Xiaofei He and Partha Niyogi. Locality preserving projections. In *Advances in neural information processing systems*, pages 153–160, 2004.
- Md Rashedul Islam, Aklima Akter Lima, Sujoy Chandra Das, MF Mridha, Akibur Rahman Prodeep, and Yutaka Watanobe. A comprehensive survey on the process, methods, evaluation, and challenges of feature selection. *IEEE Access*, 2022.
- Soham Jana, Henry Li, Yutaro Yamada, and Ofir Lindenbaum. Support recovery with stochastic gates: Theory and application for linear models. *arXiv preprint arXiv:2110.15960*, 2021.
- Eric Jang, Shixiang Gu, and Ben Poole. Categorical reparameterization with Gumbel-softmax. *arXiv preprint arXiv:1611.01144*, 2016.
- Eric Jang, Shixiang Gu, and Ben Poole. Categorical reparameterization with Gumbel-Softmax. *arXiv preprint arXiv:1611.01144*, 2017.
- Andras Janosi, William Steinbrunn, Matthias Pfisterer, and Robert Detrano. Heart Disease. UCI Machine Learning Repository, 1988. DOI: 10.24432/C52P4X.
- Ron Kohavi and George H John. Wrappers for feature subset selection. *Artificial intelligence*, 97(1-2):273–324, 1997.
- Vipin Kumar and Sonajharia Minz. Feature selection: A literature review. *Smart Comput. Rev.*, 4:211–229, 2014.

- Shahar Levy, Maria Lavzin, Hadas Benisty, Amir Ghanayim, Uri Dubin, Shay Achvat, Zohar Brosh, Fadi Aeed, Brett D Mensh, Yitzhak Schiller, et al. Cell-type-specific outcome representation in the primary motor cortex. *Neuron*, 107(5):954–971, 2020.
- David D Lewis. Feature selection and feature extraction for text categorization. In *Speech and Natural Language: Proceedings of a Workshop Held at Harriman, New York, February 23-26, 1992*, 1992.
- Fan Li, Yiming Yang, and Eric P Xing. From lasso regression to feature vector machine. In *Advances in Neural Information Processing Systems*, pages 779–786, 2006.
- Jundong Li, Kewei Cheng, Suhang Wang, Fred Morstatter, Robert P. Trevino, Jiliang Tang, and Huan Liu. Feature selection. *ACM Computing Surveys*, 50(6):1–45, dec 2017. doi: 10.1145/3136625. URL <https://doi.org/10.1145/3136625>.
- Wei Li, Jianxing Feng, and Tao Jiang. IsoLasso: a LASSO regression approach to RNA-Seq based transcriptome assembly. In *International Conference on Research in Computational Molecular Biology*, pages 168–188. Springer, 2011.
- Lianjia. Housing price in Beijing, 2017. URL <https://www.kaggle.com/datasets/ruiqurm/lianjia>.
- Ofir Lindenbaum, Yariv Aizenbud, and Yuval Kluger. Probabilistic robust autoencoders for outlier detection. *arXiv preprint arXiv:2110.00494*, 2021a.
- Ofir Lindenbaum, Moshe Salhov, Amir Averbuch, and Yuval Kluger. L0-sparse canonical correlation analysis. In *International Conference on Learning Representations*, 2021b.
- Ofir Lindenbaum, Uri Shaham, Erez Peterfreund, Jonathan Svirsky, Nicolas Casey, and Yuval Kluger. Differentiable unsupervised feature selection based on a gated laplacian. *Advances in Neural Information Processing Systems*, 34:1530–1542, 2021c.
- Yun Liu, Po-Hsuan Cameron Chen, Jonathan Krause, and Lily Peng. How to read articles that use machine learning: users’ guides to the medical literature. *Jama*, 322(18):1806–1816, 2019.
- Christos Louizos, Max Welling, and Diederik P Kingma. Learning sparse neural networks through l_0 regularization. *arXiv preprint arXiv:1712.01312*, 2017.
- Chris J Maddison, Andriy Mnih, and Yee Whye Teh. The concrete distribution: A continuous relaxation of discrete random variables. *arXiv preprint arXiv:1611.00712*, 2016.
- Andrew Miller, Nick Foti, Alexander D’Amour, and Ryan P Adams. Reducing reparameterization gradient variance. In *Advances in Neural Information Processing Systems*, pages 3708–3718, 2017.
- Hanchuan Peng, Fuhui Long, and Chris Ding. Feature selection based on mutual information criteria of max-dependency, max-relevance, and min-redundancy. *IEEE Transactions on pattern analysis and machine intelligence*, 27(8):1226–1238, 2005.
- Juha Reunanen. Overfitting in making comparisons between variable selection methods. *Journal of Machine Learning Research*, 3(Mar):1371–1382, 2003.
- Uri Shaham, Ofir Lindenbaum, Jonathan Svirsky, and Yuval Kluger. Deep unsupervised feature selection by discarding nuisance and correlated features. *Neural Networks*, 152:34–43, 2022.
- Hajin Shim, Sung Ju Hwang, and Eunho Yang. Joint active feature acquisition and classification with variable-size set encoding. *Advances in neural information processing systems*, 31, 2018.
- Le Song, Alex Smola, Arthur Gretton, Karsten M Borgwardt, and Justin Bedo. Supervised feature selection via dependence estimation. In *Proceedings of the 24th international conference on Machine learning*, pages 823–830. ACM, 2007.
- Le Song, Alex Smola, Arthur Gretton, Justin Bedo, and Karsten Borgwardt. Feature selection via dependence maximization. *Journal of Machine Learning Research*, 13(May):1393–1434, 2012.
- Ram Dyuthi Sristi, Gal Mishne, and Ariel Jaffe. Disc: Differential spectral clustering of features. In *Advances in Neural Information Processing Systems*, 2022.
- Gary Stein, Bing Chen, Annie S Wu, and Kien A Hua. Decision tree classifier for network intrusion detection with ga-based feature selection. In *Proceedings of the 43rd annual Southeast regional conference-Volume 2*, pages 136–141. ACM, 2005.
- Ryan Thompson, Amir Dezfouli, and Robert Kohn. The contextual lasso: Sparse linear models via deep neural networks, 2023.
- Robert Tibshirani. Regression shrinkage and selection via the lasso. *Journal of the Royal Statistical Society. Series B (Methodological)*, pages 267–288, 1996.

- Yutaro Yamada, Ofir Lindenbaum, Sahand Negahban, and Yuval Kluger. Feature selection using stochastic gates. In *International Conference on Machine Learning*, pages 10648–10659. PMLR, 2020.
- Junchen Yang, Ofir Lindenbaum, and Yuval Kluger. Locally sparse neural networks for tabular biomedical data. In *International Conference on Machine Learning*, pages 25123–25153. PMLR, 2022.
- Mingzhang Yin, Nhat Ho, Bowei Yan, Xiaoning Qian, and Mingyuan Zhou. Probabilistic best subset selection via gradient-based optimization, 2022.
- Jinsung Yoon, James Jordon, and Mihaela van der Schaar. Invase: Instance-wise variable selection using neural networks. In *International Conference on Learning Representations*, 2018.
- Zexuan Zhu, Yew-Soon Ong, and Manoranjan Dash. Wrapper-filter feature selection algorithm using a memetic framework. *IEEE Transactions on Systems, Man, and Cybernetics, Part B (Cybernetics)*, 37(1):70–76, 2007.

A Theoretical Proofs

Proof of Theorem 1: Firstly, the optimal solution for Eq. 1 lies in the feasible solution space for Eq. 2. Secondly, Eq. 2 attains its optimal value at the extreme values of the Bernoulli parameters $\pi(z)$. We refer the reader to Yin et al. [2022] for detailed proof.

Proof of Theorem 3:

Step 1: When we consider $L(\cdot, \cdot)$ to be a mean squared loss, the solution to the optimization problem in Eq. 7 and Eq. 2 will be given by their respective MMSE (minimum mean squared error) estimates. These are given by,

$$f_{\theta^*}(x \odot s') = E[Y|X = x, S' = s'] \quad (11)$$

$$f_{\theta^*}(x \odot s'(z)) = E[Y|X = x, Z = z, S'(z) = s'(z)] \quad (12)$$

where the feature selection vector s' and contextual feature selection vector $s'(z)$ will be sampled from a constrained space.

Step 2: Relaxing f_{θ} to be a linear function $f_{\theta}(x) = \theta^T x$, the above MMSE estimates are further reduced to

$$\begin{aligned} E[Y|X = x, S' = s'] &= f_{\theta^*}(x \odot s') \\ &= \theta^{*T}(x \odot s') \\ &= (x \odot \theta^*)^T s' \end{aligned} \quad (13)$$

$$\begin{aligned} E[Y|X = x, Z = z, S'(z) = s'(z)] &= f_{\theta^*}(x \odot s'(z)) \\ &= \theta^{*T}(x \odot s'(z)) \\ &= (x \odot \theta^*)^T s'(z) \end{aligned} \quad (14)$$

Step 3: We now average the estimates given in Eq. 13 and Eq. 14 across S' and $S'|Z = z$ respectively.

$$E[Y|X = x] = E_{S'}(x \odot \theta^*)^T s' = (x \odot \theta^*)^T \pi_{\text{stg}}^* \quad (15)$$

$$\begin{aligned} E[Y|X = x, Z = z] &= E_{S'(z)}(x \odot \theta^*)^T s'(z) \\ &= (x \odot \theta^*)^T \pi^*(z) \end{aligned} \quad (16)$$

Step 4: We now project the MMSE estimate of c-STG onto the space of contextual-feature selection vectors that remain constant across contextual variables. This is given by

$$\begin{aligned} E_Z E[Y|X = x, Z = z] &= E_Z(x \odot \theta^*)^T \pi(z) \\ &= (x \odot \theta^*)^T E_Z \pi^*(z) \end{aligned} \quad (17)$$

Step 5: This solution should be equivalent to solving the STG problem as it restricts the stochastic gates to be constant over z . Comparing the two equations Eq. 15 and Eq. 17, we get $\pi_{\text{stg}}^* = E_Z[\pi^*(z)]$.

Proof of Theorem 4: This follows from the proof of Theorem 3 by replacing Eq. 15 and Eq. 16 with the following two equations respectively:

$$E[Y|X = x] = E_{S'}(x \odot \theta^*)^T s' = (x \odot \theta^*)^T \mu_{\text{stg}}^* \quad (18)$$

$$\begin{aligned} E[Y|X = x, Z = z] &= E_{S'(z)}(x \odot \theta^*)^T s'(z) \\ &= (x \odot \theta^*)^T \mu^*(z) \end{aligned} \quad (19)$$

B Implementation Details

In selecting model architecture, we aim to maintain simplicity, interpretability, and linearity whenever feasible. When possible, we retained the same hypernetwork and prediction model architecture across various methods. For the hypernetwork, we conducted experiments with one and two hidden layers, while for the prediction networks, we explored options ranging from zero (linear) to two hidden layers. The final model architectures for each of the datasets are mentioned below in their respective paragraphs. To determine the best hyperparameters, namely the learning rate (η) and regularization coefficient (λ), we performed a grid search over the following values: $\eta \in \{1e^{-1}, 5e^{-2}, 1e^{-2}, 5e^{-3}, 1e^{-3}, 5e^{-4}, 1e^{-4}\}$ and $\lambda \in \{1, 5e^{-1}, 1e^{-1}, 5e^{-2}, 1e^{-2}, 5e^{-3}, 1e^{-3}\}$. The same set of values were used for the grid search across all the datasets. The selection of model parameters/hyperparameters was based on preventing issues like underfitting and overfitting and ensuring optimal 5-fold cross-validated performance.

Simulated Dataset: The hypernetwork \tilde{h}_ϕ has two fully connected layers, with 100 and 10 neurons, respectively. We employed ReLU as the activation function after the first layer and Sigmoid activation after the last layer. For the prediction model, we used two fully connected layers, with 10 and 10 neurons, respectively, and their corresponding nonlinearities, ReLU and sigmoid.

MNIST: For the MNIST dataset, the configuration of the hypernetwork \tilde{h}_ϕ differs, possessing two layers with 64 and 128 neurons. The same ReLU and Sigmoid activation sequence is maintained. The prediction model consists of layers with 128 and 64 neurons, coupled with the ReLU followed by Sigmoid activations.

Housing: We employed a hypernetwork architecture similar to the one used in the MNIST example. However, we used a linear model to predict house prices in this case. We divided the data into 10 train, validation, and test splits and conducted a grid search on η and λ for each split. We then selected the hyperparameters with the best validation performance.

Heart disease The full list of features includes: chest pain type (cp), resting blood pressure (resttbps), serum cholesterol levels (chol), fasting blood sugar (fbs), resting electrocardiographic results (restecg), maximum heart rate achieved (thalach), exercise-induced angina (exang), ST depression induced by exercise (oldpeak), the slope of the peak exercise ST segment (slope), the number of major vessels colored by fluoroscopy (ca), and thalassemia (thal). Among these features, cp, restecg, slope and that are categorical and hence are converted to one hot encoding vectors for feeding them into the prediction model. The hypernetwork and prediction model have one hidden layer with 1000 neurons and 10 neurons, respectively, with sigmoid activation on their last layer. We conducted a grid search on η and λ from the range of values mentioned in the MNIST example.

Neuroscience: The model was trained using 5-fold cross-validation with separate sets of trials for training, parameter tuning, and testing. We conducted a grid search on different learning rates and regularization parameters ranging from 0.0005 to 0.1 and for number of hidden units of the hypernetwork ranging from 10 to 1000 units. Overall, for the hypernetwork, we used a single hidden layer of 500 units, a learning rate of 0.005, and a regularization weight of 0.005, where the prediction network consisted of six hidden layers of 500, 300, 100, 50, and 2 units. Figure 7 presents examples of raw activity of 6 cells, selected as relevant for outcome prediction. The average activity (across trials) of these cells is plotted in 6. In Figure 7, each heat map depicts the activity of a single cell for all trials as a function of time. Trials were sorted by outcome (failed trials on top, successful trials on bottom). Cells 1, 5, and 6 become active on failed trials approximately 2 seconds after the tone, whereas cells 2, 3, and 4 become active on successful trials. This unique dynamics of a small sub-population reporting outcome was one of the main biological findings in Levy et al. [2020].

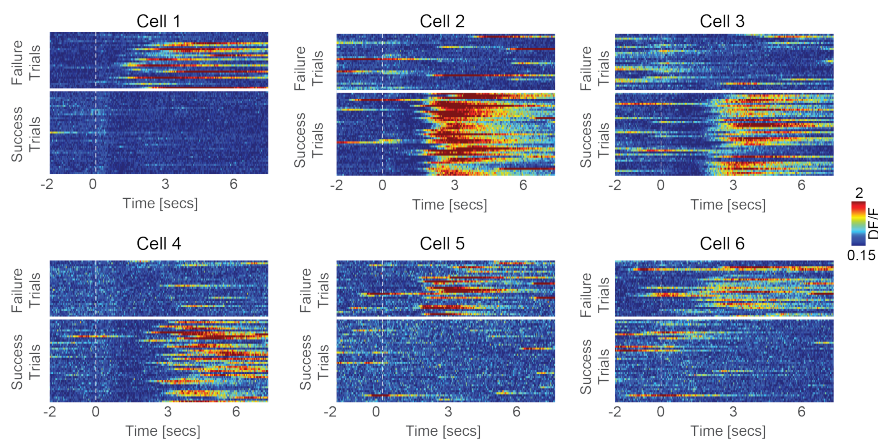


Figure 7: 2-Photon cellular imaging data set - neuronal activity across trials of cells selected as relevant to outcome prediction (matching cells presented in Figure 6)

C Additional Experiments

Sparsity-Driven Performance Analysis: We evaluate the performance of c-STG as a function of the number of selected features in the model, i.e., sparsity. Our analysis uses the MNIST example, as described in section 4. To

Table 2: Comparison of a number of features selected on XOR, MNIST, Housing, and heart disease datasets. **Bold** indicates least number of selected features and underline indicates second-best.

	XOR	MNIST	Heart disease	Housing
LASSO	18.8 (0.87)	621.70 (4.77)	13.6 (1.11)	8.0 (0.0)
with context	21.5 (0.92)	627.5 (3.26)	16.9 (0.7)	10.0 (0.0)
STG	6.60 (1.50)	585.40 (3.77)	16.60 (2.65)	8.00 (0.00)
with context	4.20 (0.40)	148.80 (2.64)	18.00 (4.15)	8.0 (0.0)
Contextual LASSO	5.33 (7.25)	357.72 (8.88)	11.79 (3.66)	5.43 (0.29)
AFS	5.40 (4.27)	290.00 (20.00)	8.00 (5.48)	<u>2.70</u> (0.64)
INVASE	9.85(1.47)	376.49(12.30)	9.12(1.85)	-
c-STG (Ours)	3 (0)	<u>247.25</u> (10.84)	9.69 (0.81)	2.70 (0.42)

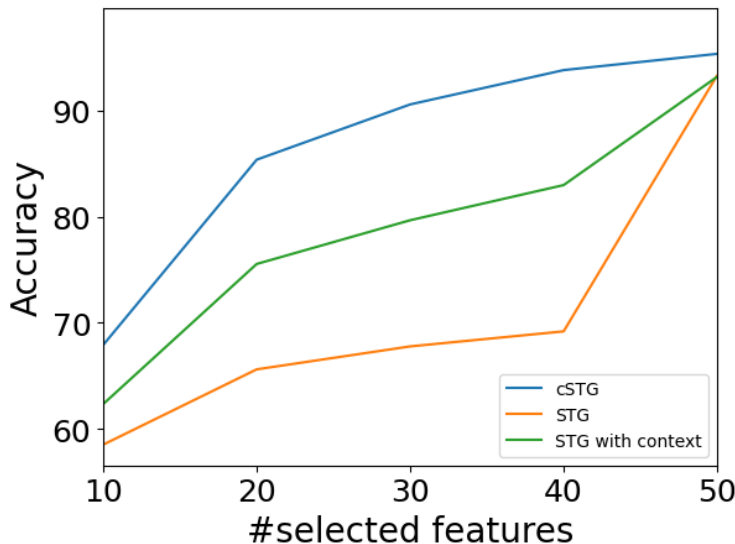


Figure 8: Comparing the performance variations of cSTG, STG, and STG with context with respect to different sparsity levels on the MNIST dataset.

perform this analysis, we varied the regularization coefficient, λ , in a way that controlled the sparsity level within the range of 10 to 50. It is worth noting that for STG with context, we only counted the explanatory features corresponding to pixels and not the eight additional contextual features (one-hot encoding) representing the angle. Figure 8 illustrates the performance of three models, c-STG, STG, and STG, with context, as the sparsity level increases. This demonstrates that c-STG has superior performance compared to both STG with context and STG alone, indicating that c-STG, with its contextual information and sparse representation, outperforms the other models for varying numbers of selected features.

Comparison of Discrete Contextual Model Training: When focusing on deriving insights from specific contextual features, training separate models for each specific context is a viable strategy. However, it is crucial to understand that this strategy is only applicable when the contextual variables are categorical and not continuous. Although straightforward, this method brings its own challenges, particularly when the dataset at hand is limited in size. In such cases, each model only gets to train on a subset of data corresponding to its designated context. We shed light on the consequences of this approach using the modified MNIST dataset, as elaborated in Section 4. Our exploration involved comparing two methodologies: 1) individually training eight models for each context using STG and 2) employing our c-STG to create a unified model for all contexts. To assess the efficiency of these approaches, we varied the number of training samples and captured the results in Fig. 9.

Comparatively, our c-STG model offers a compelling advantage. Instead of segregating data by context, it utilizes the entirety of the dataset, benefiting from the diverse range of contexts. A direct contrast in terms of model parameters reveals that while training separate models for each discrete context demands 876,688 parameters, the c-STG model operates with a lean set of 218,834 parameters. The reduced parameter count in c-STG does not compromise performance; in fact, it underscores c-STG’s prowess in delivering enhanced outcomes with fewer parameters.

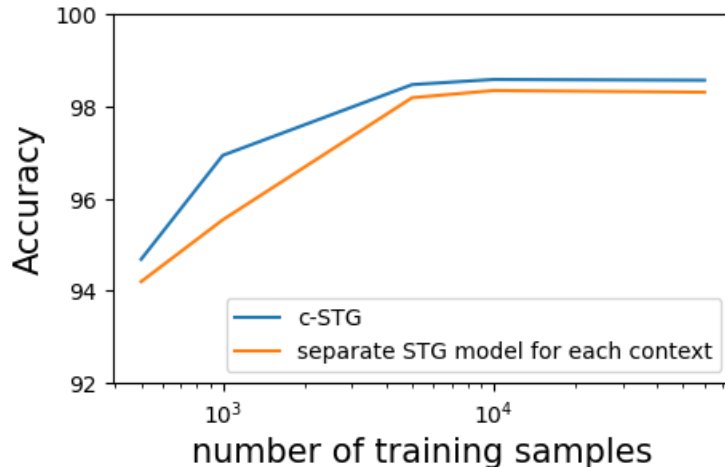


Figure 9: Comparison between training separate models for different values of categorical context variables and a single c-STG model on the modified MNIST dataset in section 4, as a number of training samples varies.

Feature Selection Across Models: We present a comparative analysis detailing the number of features chosen by each method whose prediction performance is reported in Table 1. A notable observation is that c-STG has fewer number of selected features and ranks either as the best or second-best in performance evaluation as demonstrated in Table 1. The prediction model (with context) and CEN are excluded, as no sparsity constraint is imposed on the explanatory features to perform the prediction task.

D Compute details

We trained all networks using CUDA-accelerated PyTorch implementations on a NVIDIA Quadro RTX8000 GPU.